# Magnetic field and temperature dependence of magnetic flux creep in *c*-axis-oriented $YBa_2Cu_3O_7$ powder

Youwen Xu, M. Suenaga, A. R. Moodenbaugh, and D. O. Welch
*Department of Applied Science, Brookhaven National Laboratory, Upton, New York 11973*
(Received 9 June 1989)

Creep of magnetic flux lines in a *c*-axis-oriented powder specimen of $YBa_2Cu_3O_7$ was measured at temperatures of $5<T<50$ K for fields in the range $0.1<H<4.0$ T. Under most conditions, the magnetization $M(T,H)$ was found, after sufficiently long times $t$, to decrease linearly with $\ln t$. But at higher temperatures, this linearity was not observed up to $t\simeq 1.2\times 10^4$ sec. An *apparent* flux-pinning potential $U_0^*$ can be calculated using the relationship $U_0^*=kT\{dM/[M\,d(\ln t)]\}^{-1}$. The value of $U_0^*$ at 1.0 T was found to vary from $\sim$20 to $\sim$130 meV at 5 and 35 K, respectively, and also to increase with $H$. These results are not consistent with the expected temperature dependence of the true pinning potential $U_p$, and the difficulties in the use of the above relationship to determine $U_p$ for $YBa_2Cu_3O_7$ are identified.

## I. INTRODUCTION

Soon after the discovery of high-temperature oxide superconductors, Müller *et al.*[1] found a large relaxation in the magnetization of $(La,Ba)_2CuO_4$ and argued that this behavior was a consequence of a superconducting glassy state. Following this, extensive studies of flux creep, mostly on $YBa_2Cu_3O_7$, were carried out by a number of groups.[2–11] Particularly, based on a study of magnetic relaxation of a single crystal of $YBa_2Cu_3O_7$, Yeshurun and Malozemoff[6] pointed out that the result could be interpreted as a consequence of classical thermally activated flux creep (originally proposed by Anderson[12]). (Independently, Dew-Hughes has also proposed a possibility of large thermally activated flux creep in these oxides.[13]) Using Bean's critical-state model,[14] the flux-pinning potential $U_p$ in a $YBa_2Cu_3O_7$ was estimated to be $\sim$20 meV for a small applied magnetic field parallel to the $c$ axis ($\mathbf{H}\|\mathbf{c}$).[8] (Note that this is a revised value from that found in Ref. 6.) More recently, Griessen *et al.*[10] also reported that $U_p\simeq 25$ meV for a highly textured thin film of $YBa_2Cu_3O_7$ in 1.0 T and $\mathbf{H}\|\mathbf{c}$. They have also reanalyzed the flux creep data of Yeshurun and Malozemoff[6] in accordance with their theory of flux creep and found $U_p\simeq 65$ meV.[15,16] However, in conflict with the above-mentioned values, Kes *et al.*[9] determined $U_p$ to be $\sim$1 eV in a $YBa_2Cu_3O_7$ film. This value was determined, utilizing measurements of the ac resistance of a thin film at high temperatures, by application of a model[17,18] based on flux line pinning at the twin boundaries. Furthermore, based on dc resistivity measurements, Palstra *et al.*[19] reported that the potential (activation) energies in a single crystal of $YBa_2Cu_3O_7$ are much greater ($\sim$1 to 17 eV depending on applied magnetic fields) than those previously reported. In addition, they found that $U_p$ is a strongly decreasing function of $H$. More recent studies by others,[20–22] as well as Palstra *et al.*,[23] have reexamined the activation energies $U_p$ determined from resistivity measurements. In these analyses, the temperature dependence of $U_p$ as well as nonlinearity in the variation of the potential with the force on a flux line[21] (see Sec. II) were introduced, and the values of $U_p$ which were obtained were approximately 1–4 eV (for $H=1$–4 T) in $YBa_2Cu_3O_7$. Finally, Nikolo and Goldfarb[24] reported $U_p$ for grain boundaries of $\sim$12 eV ($H=0$) and $\sim$1.2 eV ($H=10$ Oe) by measuring the frequency shift of the susceptibility $\chi''$ as a function of temperature for a polycrystalline $YBa_2Cu_3O_7$.

It is notable that, in the above review, the estimated values of $U_p$ can vary by nearly three orders of magnitude depending on how they are determined. Here, we report an analysis of creep measurements in pure $YBa_2Cu_3O_7$ in an attempt to clarify this large discrepancy. The result is discussed in terms of a model for flux creep by Beasley *et al.*[25] as well as of more recent theoretical developments on the flux creep.[9,15,16]

## II. THEORETICAL BACKGROUND

### A. The critical state model

Before summarizing the theories of the flux creep in the type-II superconductors, we restate the basis for the critical-state model since this model is often used to analyze the measurement of magnetic hysteresis and flux creep in the type-II superconductors.

The basic assumption of the critical-state model is that a superconductor is capable of sustaining *virtually* lossless currents up to a critical current density $J_c(B)$, but not beyond.[14,26] If the magnitude of the current flow throughout the entire specimen is $J_c(B)$, it is said to be in a "critical state." It is assumed that there exists a relationship $J_c(B)$ such that the critical current is solely determined by $B$ at any point in the specimen. Although this model is on many occasions associated with $J_c(B)$ being independent of $B$ as originally proposed by Bean,[14] the dependence of $J_c$ on $B$ can be a more general function

 

of $B$ as shown by Fietz *et al.*[26] Bean's model is particularly useful for $H \gg H_p$, where $H_p$ is the external field at which the magnetic field penetrates throughout the specimen. In most applications of the critical-state model, the equilibrium (or reversible) magnetization $M_r$ is not included. This is a useful approximation only for materials with very high current densities. On the other hand, the equilibrium magnetization cannot be neglected when the nonequilibrium (irreversible) magnetization becomes comparable to the reversible portion, as in the case in the oxides at high temperatures.

It must be emphasized that the critical state is very vaguely defined, e.g., "sustaining *virtually* lossless current , . . . ," as mentioned earlier. This inexact description is acceptable for the high-$J_c$ practical metallic superconductors, since flux creep is generally very slow in these materials. For example, the reduction in magnetization at 0.3–2.0 T at 4.5 K is less than a few percent in a 3-h period for state-of-the-art NbTi and $Nb_3Sn$ wires.[27] On the other hand, flux creep can result in a 10–35 % or greater reduction in magnetization in the same period for a $YBa_2Cu_3O_7$ specimen. Thus, in cases where magnetization continues to decrease it is impossible to determine at what time the critical state is established in a given specimen. In this study, *for convenience,* we assume that the critical state is established when the change in magnetization becomes linear with $\ln t$ and the creep rates for increasing and decreasing $H$ are approximately equal.

A final aspect of the critical-state model which should be kept in mind is the fact that the model is likely to be valid at magnetic fields substantially greater than the penetration field $H_p$ (at which the specimen is fully penetrated by the field). Although the model can, in principle, be applied for $H \simeq H_p$ or $H < H_p$, in these low-field regions the magnetic field gradient $\nabla B$ is steepest and varies rapidly with depth in the specimen. Thus in these cases it may be difficult to ascertain the establishment of the critical state. On the other hand, at higher fields, $\nabla B$ is a much more slowly varying function of the position, and the critical state is likely to be easily established. Furthermore, the establishment of the critical state (which is based on the assumptions stated above) can easily be checked by observing whether the condition $|\nabla B|^+ \simeq |\nabla B|^-$ is established (or, in our case, the conditions for the rates of flux creep, $R^+ \simeq R^-$), where $+$ and $-$ indicate these values for the case of increasing and decreasing field at a given value of $H$. Another benefit of making the creep measurements at higher fields ($H \gg H_p$) is the fact that the specimen is thoroughly penetrated by magnetic flux lines so that the effects of demagnetization due to nonideal specimen shapes become negligible.

### B. Flux creep

The first detailed theoretical analysis of flux creep in type-II superconductors, given by Beasley *et al.*[25] in 1969, will be summarized here. More recent developments, particularly those by Hagen and co-workers[15,16] which are said to be applicable up to higher temperatures, are briefly reviewed.

According to the critical-state model, as shown by Freidel *et al.*,[28] the driving force on the flux lines arising from the gradient of $B$ in a superconductor placed in an an applied field $H$ is given by $F = \gamma BJ/c = -\gamma B \nabla B/4\pi$, where $\gamma = \partial H(B)/\partial B$. The gradient $\nabla B$ is established due to the fact that the flux lines are pinned against potential barriers in the specimen. At $T > 0$, these can creep along the gradient by thermally activated motion between pinning sites at a rate of

$$\nu = \nu_0 e^{-U/kT} , \tag{1}$$

where $\nu_0$ is an attempt frequency and $U$ is an effective pinning energy which depends upon the driving force $F \propto B \nabla B$. A linear approximation to this dependence,

$$U(F) = U_p - FVX ,$$

is often used[12] where $U_p$ is the height of the energy barrier (or pinning potential) at $F = 0$, and $V$ and $X$ are the activation volume and the width of the barrier, respectively. By solving the continuity equation for conservation of flux, $\partial B/\partial t = -\nabla \cdot \mathbf{D}$, for cylindrical geometry where

$$D = -(\nabla B/|\nabla B|) B w \nu_0 e^{-U(B, |\nabla B|/kT)}$$

and $w$ is a distance which a moving flux bundle travels per jump, it was found[25] that the total flux $\phi$ in the specimen as a function of $t$ is given by

$$\phi = \phi_0 - A \ln(t/t_0) , \tag{2}$$

where $t_0$ is an arbitrary reference time, $A$ is a factor independent of $t$, and $\phi_0$ is $\phi(t_0)$. Then, the creep rate $R'$ is given by

$$R' \equiv d\phi/d \ln t = -(\tfrac{1}{3})\pi k T \rho^3 (\partial U/\partial |\nabla B|)^{-1}(1 \pm \delta) , \tag{3}$$

where $\rho$ is the radius of the cylindrical specimen and $\delta$ (assumed $\ll 1$) is a function of $\nabla B$ and $\partial U/\partial |\nabla B|$. The $\pm\delta$ accounts for the two cases $R'$ for increasing or decreasing $H$. The calculation was also based on the assumption that $U/kT \gg 1$.

Equation (3) can be reduced to a form suitable for obtaining an apparent pinning potential $U_0^*$ from the measured magnetization. Noting that

$$(\phi/\pi\rho^2) = \bar{B} = H + 4\pi M ,$$

where $M$ is the irreversible portion of the magnetization, and that the screening current density, and thus the magnetization $M$, is proportional to the flux gradient $\nabla B$, Eq. (3) becomes

$$\frac{1}{M}\frac{dM}{d \ln t} = -\frac{kT}{U_0^*} . \tag{4}$$

$U_0^* \equiv -|\nabla B|(\partial U/\partial |\nabla B|)$ is an apparent pinning potential whose relationship to the true pinning potential $U_p$ depends upon the nature of the $U$ versus driving-force relation, which has customarily been assumed to be linear. It should be noted that Beasley *et al.*[25] correctly pointed out that this is almost certainly not the case, and $U$ is more realistically represented as shown in Fig. 1. We

have made explicit calculations for a wide variety of assumed shapes and spacings for potential wells, ranging from closely spaced double wells to widely spaced isolated wells, with shapes ranging from very sharp to very flat, and the results show that to a good approximation

$$U(B,\nabla B)\simeq U_p(B)(1-\nabla B/\nabla B_{\max})^n \quad (5)$$

with $\frac{3}{2}<n<2$, where $\nabla B_{\max}$ corresponds to the maximum force which the pinning potential can sustain in the absence of thermal activation, i.e., $\nabla B_{\max}=\nabla B(T=0\text{ K})$. Thus, the apparent pinning potential $U_0^*$, which appears in Eq. (4), is given by

$$U_0^*\simeq nU_p\left|\frac{\nabla B}{\nabla B_{\max}}\right|\left[1-\frac{\nabla B}{\nabla B_{\max}}\right]^{(n-1)} . \quad (6)$$

Note that only if the potential versus driving-force curve [Eq. (5)] is linear ($n=1$), and then only when $J_c(T)\simeq J_c(0)$ so that $\nabla B/\nabla B_{\max}\simeq 1$, does $U_0^*$ equal the true pinning potential $U_p$. Our model calculations show that $n>1$ is more realistic than $n=1$, so that $U_0^*$ is expected to be smaller (perhaps by a large factor) than $U_p$, as first pointed out by Beasley *et al.*[25] (The apparent pinning potential $U_0^*$ from Eq. (4) is related to the apparent pinning potential $U_0$ of Beasley *et al.*,[25] shown in Fig. 1, by

$$U_0=U+U_0^*$$
$$\simeq U_0^*[1+(n-1)(\nabla B/\nabla B_{\max})]/n(\nabla B/\nabla B_{\max}) .$$

The two coincide only at $\nabla B\simeq\nabla B_{\max}$; i.e., when $J_c(T)\simeq J_c(0)$.)

Recently, based on a model of granular superconductivity, Tinkham and Lobb[29] arrived at a relationship between a pinning potential and creep rate which is identical to Eq. (4). In addition, Hagen and Griessen[15,16,30] have also pointed out that Eq. (2) is nonphysical for the limits of $t\to 0$ and $t\to\infty$ and proposed an expression (based on the assumption of a linear potential versus driving-force curve)

$$M(t)=M_0[1-(kT/U_p)\ln(1+t/\tau_0)] \quad (7)$$

for $M/M_0>0.05$, where $M_0=M(t=0)$ and

$$M(t)=M_0(2kT/U_p)\exp[-2e-U_p/kT(t/\tau_0)] \quad (8)$$

for $M/M_0<0.05$. Here $\tau_0$ is a relaxation time and $10^{-6}\le\tau_0\le 10^{-12}$ (see Refs. 15 and 16). These relationships are based on a Monte Carlo simulation,[30] without the restriction of $U/kT\gg 1$. Then, in the most readily accessible time spans for the experiments, the barrier height is expressed as

$$U_p\simeq -kT\left[\left[\frac{1}{M_0}\frac{dM}{d\ln t}\right]^{-1}+\ln(t_0/\tau_0)\right] , \quad (9)$$

where $t_0$ is the time of the first measurement after setting $H$. It was noted by Hagen and co-workers.[15,16] that $\tau_0$ is uncertain, but argued that the error due to this uncertainty is approximately 10% since it is in a logarithmic term. Then, Eq. (9) is essentially identical to Eq. (4) except the magnetization $M_0=M(t_0)$ in Eq. (9) is its value at $t=t_0$ while, in Eq. (4), $M$ is time dependent, i.e., $M(t)$. We will show later that this difference is a relatively minor one in most cases. Thus, in the following we analyze the present creep data according to Eq. (4). It should also be pointed out that the pinning potential, which is calculated using Eqs. (7)–(9), is a potential similar to $U_0$ or $U_0^*$ as defined in Fig. 1 rather than $U_p$. This is due to the fact that Hagen and co-workers[15,16] have employed a linear potential $U(\nabla B)\simeq U_p-B\nabla BVX$ rather than a nonlinear $U(\nabla B)$ as discussed earlier.

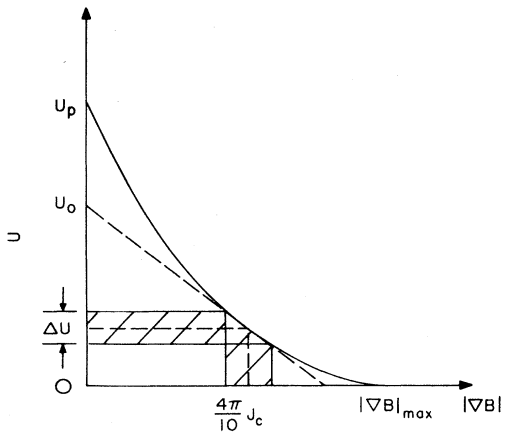


FIG. 1. A schematic representation of the pinning potential $U$ as a function of the field gradient $\nabla B$ for a constant $B$. The shaded region represents the critical-state region. [After Beasley *et al.*, Ref. 25.]

## III. EXPERIMENTAL PROCEDURES

The specimen used for this experiment was prepared by sintering appropriate amounts of $Y_2O_3$, $BaCO_3$, and CuO powders, as previously described.[31] Superconducting, structural (x-ray and neutron diffraction), and microstructural (transmission electron microscopy) characterizations indicated that this specimen is "high-quality" $YBa_2Cu_3O_7$.[31] For example, transmission electron microscopy shows that the twin-boundary spacings are, in general, very large ($\gtrsim 200$ nm) and the twin-boundary-layer thickness is approximately 1.0 nm.[32] Alloying $YBa_2Cu_3O_7$ (replacements for Cu), or removal of oxygen was found to increase the boundary layer width. This suggests that narrow boundaries are a sign of a "better" specimen. The grains of the sintered specimens are also found to be very large, e.g., $\sim 40$ $\mu$m in the $a$ or $b$ direction. The critical temperature ($T_c$) measured by ac susceptibility (200 Hz) was 90.5 K $\Delta T_c\simeq 2.5$ K, while the resistive $T_c$ was 92 K with $\Delta T_c\simeq 0.2$ K. The normal-state resistivity at 100 K was 250 $\mu\Omega$ cm.

For the measurements of magnetic properties, the sintered specimen was ground to a particle size less than $\sim 38$ $\mu$m ($-400$ mesh). The average particle size was determined to be $\sim 30$ $\mu$m by analyzing the images of the

particles from a scanning electron microscope. In order to orient the powder in the "$c$" direction, the powder was mixed in a 5-min epoxy, cast in a mold and held at $H=8$ T.[33,34] To determine the degree of orientation of the powder, a transmission Laue pattern of the composite was taken along the direction perpendicular to the $c$ axis. It exhibited very strong single-crystal-like reflection spots, although very weak rings were also observed in the background. Measurements of magnetic hysteresis and $H_{c2}$ of the composite also showed strong anisotropy in two perpendicular directions. These results indicated that the particles in the composite were predominantly aligned along the $c$ axis.

For measurements of magnetic properties, a superconducting quantum interference device (SQUID) magnetometer (Quantum Design) was used. Unless carefully established procedures were followed in measuring magnetic properties of superconductors, particularly magnetic hysteresis and flux creep, erroneous magnetic moments and creep rates could be obtained. Thus, we describe the exact procedure followed in measurements of the hysteresis and the flux creep. (1) The scan length, the distance which a specimen travels through a set of detection coils, is set at 30 mm. This relatively short travel minimizes the magnetic field variation in which a specimen travels. Variation in $H$ at this setting is estimated to be $<0.05\%$. (2) After a temperature is set, the external magnetic field is increased by small increments from zero, i.e., 0.02 T steps for $H\leq 0.1$ T, 0.05 T steps for $0.1\leq H\leq 1.0$ T, and 0.1 T steps for $H>1.0$ T. This procedure avoids an overshoot in $H$, which can also give erroneous results. Hysteresis was measured at various temperatures. (3) Flux creep was also measured during the hysteresis measurement by stopping at several magnetic field values and measuring the magnetic moment as a function of time as shown in Fig. 2. The creep data were limited to times $\lesssim 1.2\times 10^4$ sec and were taken at $H=0.1$, 0.5, 1.0, 2.0, 3.0, and 4.0 T for increasing as well as for decreasing field portions of the hysteresis. For practical reasons, the hysteresis and the creep data for $H\leq 1.0$ T, $1.0\leq H\leq 3.0$ T, and $2.0<H\leq 5.0$ T are taken separately. An example of the magnetic hysteresis curve for the specimen is shown in Fig. 2. The flux creep at each field examined ($H^{+,-}=0.1$ and 0.5 T) is clearly observable as the magnetization decreases as a function of time at a fixed $H$.

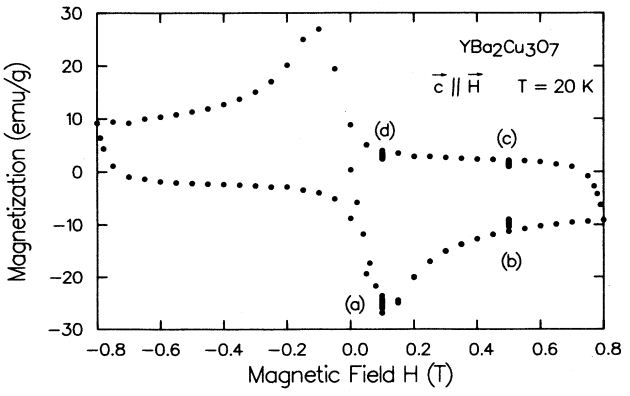


FIG. 2. A Magnetic hysteresis for a $YBa_2Cu_3O_7$ powder which are aligned in the "$c$" axis and H||"C". The markers $a$, $b$, $c$, and $d$ are the values of $H$ where the flux creep was measured.

Since both spatial and temporal uniformity in applied magnetic fields are crucial for accurate determination of magnetization and flux creep in superconductors, we have also performed the following tests to ensure that the aforementioned procedure provides accurate measurements of flux creep in these specimens. The first of these is to test the effect of the spatial magnetic field nonuniformity through which the specimen travels during a measurement cycle. In order to test this, the flux creep rate at 2 T was measured with a scan length of 20 mm, where $\Delta H\simeq 0.005\%$, instead of $\Delta H<0.05\%$ for a 30 mm scan. Although the calibration for magnetic moments is not accurate for the entire field range at this scan length (however, at 1 and 2 T, the measured moments using 20- and 30-mm scan lengths are essentially identical), the creep rates using these scan lengths may be reliably compared to determine the effect of $\Delta H$ on the rate. The result indicated that there was no observable difference in the rate, at least at the detection levels of this measurement for this study. Furthermore, we have carefully examined the shape of the wave form from the detection coils at different sensitivities since, particularly for a short scan length (e.g., 30 mm), the correctness of the measured moment is heavily dependent on the wave shape. We found no detectable deformation of the wave form in the range of sensitivity which was used for this study.

The second test is to determine the temporal stability of the measurement system consisting of a SQUID detector and a magnet system. First, using Pd and MnF (NIST standard reference specimens), we have measured the magnetic susceptibility of these materials as a function of time using the creep measurement procedure already described for magnetic fields from 0.1 to 4.0 T in increasing and decreasing cycles. Although it is not always consistent, in general, the values of the moments from our standard decreased by $\sim 0.15\%$ during a 15–30 min period and then stayed constant. In order to determine whether the variation in the susceptibility is due to the magnetic field or the SQUID system, a Hall probe was placed in the center of the magnet and the variations in $H$ with time were measured. For this measurement, a highly stable current source for the Hall probe as well as a "12-bits" digital oscilloscope were employed. The results of this test indicated that the field is stable to less than 2 G (considered to be the limit of detectability of the present field measurement system) in a 1-h period, and no overshoot was seen. Thus, we ascribe the observed variation in the susceptibility primarily to the (SQUID) system. This is likely to be due to the fact that the SQUID and the detection coils have to be disconnected every time the external field is changed and reconnected before the measurement is taken.

## IV. RESULTS AND ANALYSIS

In this section, the results of the flux creep measurements for an oriented powder of $YBa_2Cu_3O_7$ are analyzed in order to be suitable for discussion of the pinning potential as described by the theories[15,16,25] discussed earlier.

The flux creep, as observed by the measurement of magnetic moments, as a function of $\ln t$ is illustrated in Fig. 3 for several temperatures. As shown in the figure, magnetization appears to decrease linearly with $\ln t$ in most cases here. However, as temperature is increased and/or the vertical scale is expanded, deviation from this linear relationship becomes increasingly evident, particularly at short times and at low fields. These are illustrated in Figs. 4(a) and (b). In some cases, there was no linear segment in an $M(t)$ versus $\ln t$ plot, for $t \lesssim 1.2\times10^4$ sec, e.g., 4(b). In those cases for which $M(t)$ does not follow a linear $\ln t$ dependence, $M(t)$ was also plotted as a function of $\exp(-\alpha t)$ as suggested by Hagen and co-workers.[15,16] However, we did not find a tendency for $M(t)$ to follow an exponential dependence. In fact, $M(t)$ was approximately linear with $(\ln t)^{-1}$ in these cases.

From the data as shown in Figs. 3 and 4, the creep rates $dM/d\ln t$ can be calculated and are shown as a function of temperature in Fig. 5. As shown by others,[5–8] the rate has a maximum as a function of temperature for small applied fields, e.g., $H=0.1$ T. However, for higher values of applied fields, $dM/d\ln t$ is a monotonically decreasing function of $T$ for $T \geq 5.0$ K as also observed Griessen *et al.*[10] Since $dM/d\ln t$ depends on $M$ and $dM/d\ln t$ is greatest at $H_m$, for which $M$ is a maximum ($H_m \simeq H_p$), a peak in $dM/d\ln t$ is observed as a function of $T$ if $H$ is chosen such that $H < H_m$ at the lowest temperature of the measurement. In fact, at these low values of $H$, the results of the creep measurements are less suitable than those at higher magnetic fields for determination of $U_0^*$. The linear dependence of $M$ on $\ln t$ is less accurately linear and the difference in $dM/d\ln t$

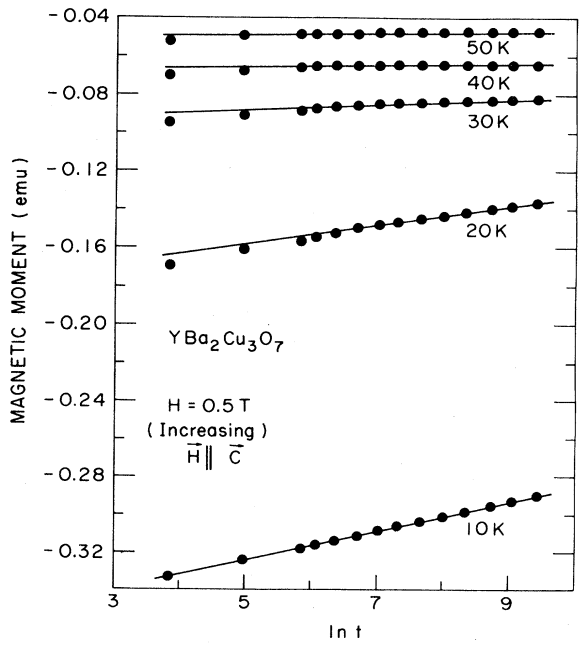


FIG. 3. An example of changes in magnetic moments with $\ln t$ at $H=0.5$ T and $T=10$, 20, 30, 40, and 50 K.

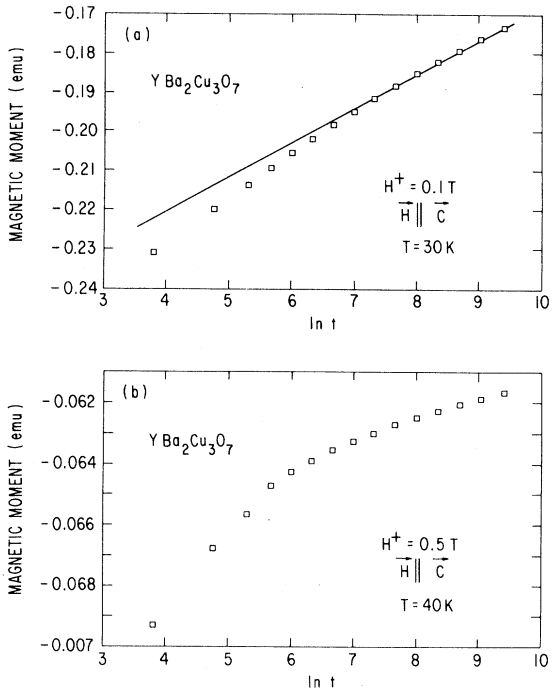


FIG. 4. Examples (a) and (b) show the decay in magnetic moments which are not linear with $\ln t$ for the entire period. In the case of (*b*) no linear segment was found.

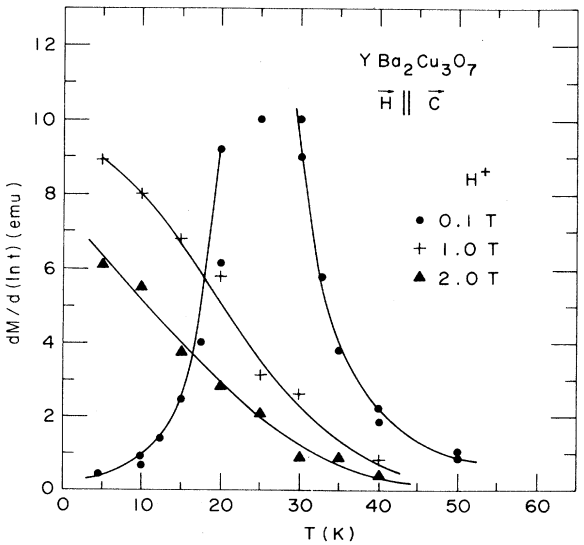


FIG. 5. Temperature dependence of $dM/d(\ln t)$ for $H=0.1$, 1.0, and 2.0 T. A peak in $dM/d\ln t$ was found when $H < H_p$ at a low temperature.

for increasing $H^+$ and decreasing $H^-$ becomes greater than for a higher value of $H$. This suggests that the critical state might not be well established under these experimental conditions for this specimen. This is perhaps due to a steep gradient in $B$ in the specimen at these low magnetic fields. For this reason, the present calculations of the pinning potential were limited to the measurements for $H \geq 1.0$ T.

In order to analyze the creep data using the theories discussed earlier, it is necessary to determine the values of the irreversible portion of magnetization, i.e., $M_{\rm irr}=(M-M_r)$, which drives the time-dependent critical-state current in the specimen. This was not explicitly treated earlier. But, for the present case, where the values of $M_{\rm irr}$ and $M_r$ are comparable, it is important to use $M_{\rm irr}$ for $M$ in Eqs. (4) and (9). First, we note the following relationship[26] assuming the critical state is established,

$$4\pi(M^+ + M^-) \simeq 2(4\pi M_r) \tag{10}$$

and

$$4\pi(M^+ - M^-) = 4\pi\Delta M = 8\pi(M^+ - M_r) \simeq \tfrac{2}{3}kJ_c\rho \ . \tag{11}$$

The first is a simple way to determine $M_r$ from a magnetic hysteresis at a given $H$ and the second is the commonly used relationship to determine $J_c$ from a magnetization measurement for a cylindrical geometry where $\rho$ is the radius of the specimen and $k$ is a constant depending on the units used. Again, + and − indicate the value of $M$ which was measured in the increasing and decreasing portion of the hysteresis, respectively. Since, as shown in Fig. 4(a) and (b), in many cases $M(t)$ is not proportional to $\ln t$ for the entire time period of a creep measurement, we will determine "instantaneous creep rate" $(1/M)(dM/d\ln t)$, rather than $[1/M(t_0)](dM/d\ln t)$. [The use of $M(t_0)$ instead of $M$ in the creep rate did not change the essential nature of the present result.] In practice, we calculate the creep rate,

$$R_i \equiv dM_{ij}/[(M_i - M_r)d(\ln t)_{ij}] \ ,$$

where

$$dM_{ij} = M_j - M_i$$

and

$$d(\ln t)_{ij} = \ln t_j - \ln t_i$$

and $i$ and $j$ are the consecutive points in the creep measurement. Here we assume $M_r$ to be time independent. In some cases, $R_i^+$ and $R_i^-$ are greatly different, and then $M_r$ as determined by Eq. (10) is not constant with $t$. However, if $M_r$ is determined using the last few points in the process of the creep measurements, i.e., $\ln t \simeq 8-10$, the value of $M_r$ is likely to be a good approximation for the reversible magnetization.

Also, in order to determine an average rate of flux creep for the increasing and decreasing portion of the hysteresis at a given applied field, we use $\langle R_i \rangle = \frac{1}{2}(R_i^+ + R_i^-)$ as shown in Ref. 25. This will eliminate $\delta$ in Eq. (3). In addition, $R_i^+$ and $R_i^-$ are used to estimate

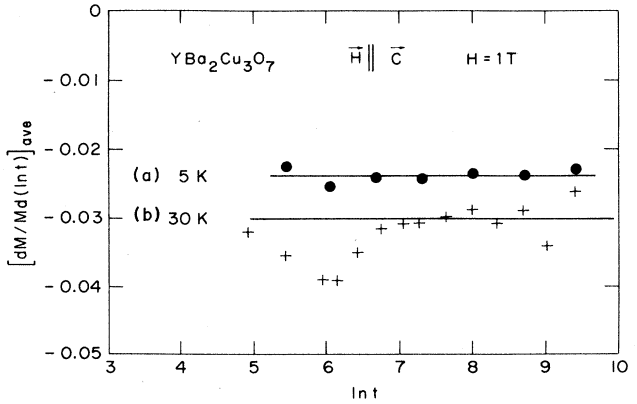


FIG. 6. The instantaneous creep rate $\langle R_i \rangle = 1/2(R_i^+ + R_i^-)$ as a function of $\ln t$. The figures such as these were used to determine $\langle R \rangle_a = (dM/Md\ln t)$ for calculating $U_0^*$.

$\delta$ as $\delta = (R_i^+ + R_i^-)/2$. It was found that the values of $\delta$ at 1.0 and 2.0 T were less than $\sim 0.15$ for all measurements except for two sets. However, significantly larger values of $\delta$ were observed at 0.1 and 0.5 T for most of the cases. Finally, the values of $\langle R_i \rangle$ are plotted as a function of $\ln t$ and examples are shown in Fig. 6. In general, $\langle R_i \rangle$ was constant in $\ln t$ for low-temperature and high-field data, e.g., Fig. 6(a). As the temperature is increased, the deviation in $\langle R_i \rangle$ from a constant value increases, particularly for small values of $\ln t$. Also $\langle R_i \rangle$ deviates significantly before establishing a constant value for a large $\ln t$ as shown in Fig. 6(b). For calculation of $U_0^*$ in Eq. (4), we used the average value $\langle R \rangle_a$, determined from plots such as Fig. 6. The solid lines in the figure indicates the values of $\langle R \rangle_a$ for these two sets of data.

From the values of $\langle R \rangle_a$, the *apparent* potential barrier $U_0^*$ for the flux motion is calculated $(U_0^* = -kT\langle R \rangle_a^{-1})$ and plotted in Fig. 7 as a function of $T$ for $H = 1.0$ and 2.0 T. The creep rates were also mea-

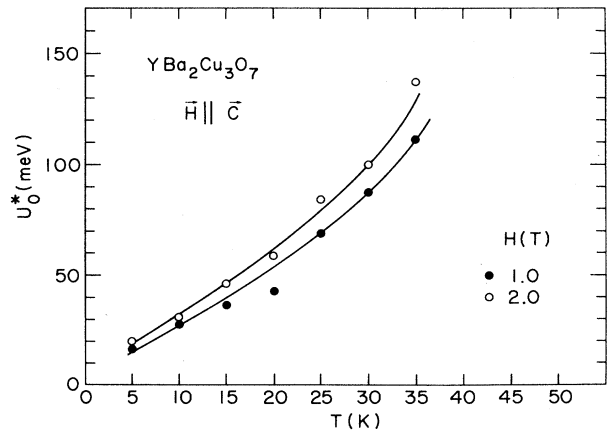


FIG. 7. The apparent flux pinning energy as a function of temperature.

TABLE I. Magnetic field dependence of the apparent pinning potential $U_0^*$ (meV).

| | $H(T)$ | | | | |
|---|---|---|---|---|---|
| $T$ (K) | 0.5 | 1.0 | 2.0 | 3.0 | 4.0 |
| 10 | 28.7 | 28.5 | 30.1 | 36.7 | 41.4 |
| 20 | 35.8 | 41.0 | 55.5 | 73 | 83 |

sured for the same specimen at 3.0 and 4.0 T for 10 and 20 K. The calculated values of $U_0^*$ for these fields are listed in Table I. The interpretation of these results are discussed in the following section.

The present measurements of $\langle R \rangle_a$ and thus $U_0^*$ for 1.0 and 2.0 T, were limited to $T \leq 35$ K due to the reduced signal and to the increased nonlinearity in the $(1/M)dM/d\ln t$ at high temperatures. In order to study the creep at higher temperatures, a specimen with large grains, and thus larger particle size, and a larger total mass than the present one ($\sim 15$ mg) is being prepared.

Finally, the widths of the magnetic hysteresis, $\Delta M(H)=(M^+ - M^-)$ [see Eq. (11)], which are proportional to critical current densities, are determined for $H=0.1$, 1.0, and 2.0 T at $t \simeq 12\,000$ sec and are plotted as a function of temperature in Fig. 8. As will be discussed later, in the interpretation of the measured $U_0^*$ it is important to find the values of $J_c(T)/J_c(0)$ and this figure is used to approximate this ratio for the present case. However, one possible difficulty in the use of $J_c$, as determined by magnetic hysteresis for $YBa_2Cu_3O_7$, is that the observed rapid decrease in $\Delta M(H)$ with increasing $T$ may be strongly influenced by the weakening of defects such as twin boundaries with increasing temperature where magnetic fields penetrate. Thus the magnetization is reduced by the subdivision of the specimen. If this is the case, the temperature dependence of $J_c(T)$ in Fig. 8 does not represent the reduction of $J_c$ due to effective "weakening" of the pinning potential by the increased thermal activation. Thus, this result may not be appropriate for use in the interpretation of $U_0^*$. However, at this point, it is not clear whether the twin boundaries are breaking down at the field and temperature ranges of the present study.

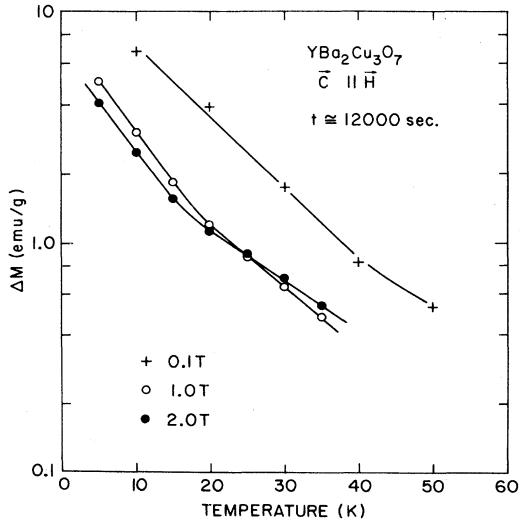


FIG. 8. The temperature dependence of the magnetic hysteresis width $\Delta M(H)$ for $H=0.1$, 1.0, and 2.0 T.

## V. DISCUSSION

Various aspects of the temperature and field dependence of the apparent barrier height $U_0^*$, which was determined as described earlier, require some discussion. First, the low-temperature values for $U_0^*$ ($\sim 20$ meV) are in good agreement with those obtained for a single crystal and for a highly-textured film by Yeshurun *et al.*[6–8] and by Griessen *et al.*,[10] respectively. However, as the temperature is increased, the values of $U_0^*$ unexpectedly and sharply increase up to $\sim 120$ meV at 35 K. If $U_0^* \simeq U_p$ (the true pinning potential), it is expected that $U_0^*$ will slowly decrease with increasing $T$ until $T \simeq T_c$ where it is expected to rapidly decrease to zero. Moreover, as shown in Table I, in the limited range of $H$ for which we have measured $U_0^*$, $U_0^*$ increases with $H$. This is in contrast to the observation made by others,[19–24] i.e., the activation energy was a strongly decreasing function of $H$ for single crystals of $YBa_2Cu_3O_7$ and Bi-Ca-Sr-Cu-O, as determined by a high-sensitivity resistance measurement. On the other hand, Yamafuji *et al.*[35] suggest a possibility for $U_p$ to increase slowly with temperature. This proposal is based on a pinning barrier which was calculated for a magnetic-flux lattice, rather than for a single flux line or a bundle of flux lines as assumed for the discussion in Sec. II. However, the predicted increase in $U_p$ with $T$ was too slow to account for the present observation.

Thus, one is forced to ask what is the significance of the apparent pinning potential $U_0^*$ as determined by the measurements of the flux creep rates combined with Eq. (4)? [Again the use of the alternate Eq. (9) for determining $U_0^*$ does not change the essential nature of Fig. 7.] A likely possible cause for this puzzling result may be found in the discussion of Fig. 1 in Ref. 25. (This figure is reproduced in our Fig. 1.) As described, the flux creep $dM/d\ln t$ or $d\phi/d\ln t$ is proportional to $(\partial U/\partial|\nabla B|)$, see [Eq. (3)] under the conditions of the experiment. At a given temperature, there will be an apparent critical current density $J_c$ and an equivalent gradient $|\nabla B_c|=4\pi J_c/10$, and the creep rate is then determined by the value of $\partial U/\partial|\nabla B|$ at $|\nabla B|_c$, as illustrated in Fig. 1. This is also equivalent to the use of the equation $U \simeq U_0 - FXV$, as is commonly done. As pointed out by Beasley *et al.*,[25] this $U_0$ is not the maximum depth of the given pinning potential $U_p$, but is simply an intersection of the tangent $(\partial U/\partial|\nabla B|)$ at $\nabla B \simeq |\nabla B|_c \simeq J_c$ and the $U$ axis. A casual observation of the figure may lead to the conclusion that the observed temperature dependence of $U_0^*$ is merely the variation of $U_0$, as shown in the figure, as the operating value of $J_c$ is decreased with increasing temperature. Furthermore, the magnetic field depen-

dence of $U_0^*$, as shown in Table I, may also be explained in a similar manner. Thus, the results shown in Fig. 7 only indicate that the maximum depth of the potential in this specimen is *greater* than $\sim 120$ meV, and this is not inconsistent with other measured values of the pinning potential.[19–24] In addition, a preliminary measurement of $U_0^*$ for a large grained and textured polycrystalline specimen of $YBa_2Cu_3O_7$ indicates a similar increase in $U_0^*$ with increasing temperature, from 10 up to 60 K and a rapid decrease beyond $\sim 60$ K.[36] This further appears to support our interpretation of the $U_0^*$ versus $T$ based on the theory by Beasley *et al.*[25] *Unfortunately*, however, a more careful examination of the steps leading to Eq. (4) indicates that there are some serious difficulties with the use of Eq. (4) for the present case in relating the creep rate $(1/M)(dM/d\ln t)$ to the pinning potential. One of these is the fact that the approximation,

$$|\nabla B_c|(\partial U/\partial|\nabla B|)_c \equiv U_0 \approx U_0^*$$

(where $U_0$ is defined in Fig. 1), is only applicable for $J_c(T) \simeq J_c(0)$ or $T \simeq 0$ K. [See the discussion following Eq. (6)]. As shown in Fig. 8, even at $T=5$ K the ratio of $J_c$ (5 K) to $J_c(0)$ at for example, 2.0 T is approximately 0.6. The above assumption, used by Beasley *et al.* in simplifying Eqs. (3) to (4) in order to obtain $U_0$, is not valid.

Perhaps, a more serious difficulty in the attempt to interpret the present result in terms of the theories discussed above, is the fact that for a wide variety of pinning potential wells leading to a curve of $U$ versus $\nabla B$ curve such as shown in Fig. 1, the intercept $U_0$ increases with increasing temperature at a nearly infinite slope at $|\nabla B|_{\max}$ or $T=0$ K instead of the near zero slope suggested by the temperature dependence of $U_0^*$ in Fig. 7;[37] i.e., these calculations would lead to a curve of $U_0^*$ versus $T$, which is concave downward rather than upward as seen in Fig. 7. Thus, at this time, it appears that the equation, which was developed to relate the flux creep to the pinning potential, is not suitable for the present case of $YBa_2Cu_3O_7$. However, it is also possible that this difficulty is partly due to the unsuitability of the specimen for a simple interpretation of magnetization, i.e., whether each particle of $YBa_2Cu_3O_7$ is behaving as a uniform single particle or a particle subdivided at the twin boundaries. In order to clarify some of the preceding problems in regard to the interpretation of the flux creep as measured by magnetization, a study of NbTi and $Nb_3Sn$ wires is being conducted.[27]

One method, which was not considered here, for analysis of the present creep data to deduce the pinning potential is to consider a distribution in energy of the pinning potential. Since the sizes and the types of the crystallographic defects in a specimen vary, the strength of the pinning potential is expected to vary from one site to another, resulting in a distribution of the pinning energy. This effect was considered by Hagen and Griessen.[38] However, for the present analysis, we have not considered this possibility since some of the observed trends in $U_p$, such as its magnetic field dependence, are unrealistic and suggest either that the present theory of the flux pinning is not applicable to the oxide or that the variations in the moment as a function of temperature are not due to uniform penetration of the flux in the specimen.

Another interesting question which is brought out by this experiment is, what are the defects which pin the flux lines in this flux creep experiment. The often discussed candidate pinning sites are the twin boundaries[17,39] in $YBa_2Cu_3O_7$. Flux decoration experiments[40,41] indicated that the flux lines are preferentially situated at the twin boundaries. This suggests that the boundaries are strong pinning sites. However, in this present experiment, the individual particles of $YBa_2Cu_3O_7$ are single grains and the twin boundaries extend across the entire particle. Also, the spacings between the boundaries are large ($\gtrsim 0.2$ $\mu$m).[31] Thus, it is *not* likely that the twin boundaries are very effective pinning sites. If this is the case, the values of $U_0^*$ measured here may possibly be that for point defects in the specimen, and for what is sometimes called "intrinsic" pinning.[40,41] This question will be addressed in detail elsewhere.

## VI. SUMMARY

The temperature and magnetic field dependence of magnetic flux creep were measured for an oriented powder of $YBa_2Cu_3O_7$. This result was used to reduce the *apparent* flux pinning potential using a relationship

$$U_0^*(T) \simeq kT(dM/Md\ln t)^{-1} .$$

It was shown, however, that it is difficult to relate the values of $U_0^*$ to the true depth of the pinning potential, $U_p$. It is also not clear at this time whether this difficulty is due to deficiency in the theories of flux creep or to the uncertainty of the behavior of the twin boundaries or possibly other defects in $YBa_2Cu_3O_7$ under magnetic fields.

## ACKNOWLEDGMENTS

The authors appreciate very valuable assistance from A. K. Ghosh and very helpful discussions with J. R. Thompson in regard to the use of the magnetometer for measuring the magnetization of superconductors. This research was performed under the auspices of the U.S. Department of Energy, Division of Materials Sciences, Office of Basic Energy Sciences under Contract No. DE-AC02-76CH00016.

[1]K. A. Müller, M. Takashige, and J. G. Bednorz, Phys. Rev. Lett. **58**, 1143 (1987).

[2]A. M. DeSantolo, M. L. Mandich, S. Sunshine, B. A. Davison, R. M. Fleming, P. Marsh, and T. Y. Kometani, Appl. Phys. Lett. **52**, 1995 (1988).

[3]T. K. Worthington, W. J. Gallagher, and T. R. Dinger, Phys. Rev. Lett. **59**, 1160 (1987).

[4]A. C. Mota, A. Pollini, P. Visani, K. A. Müller, and J. G. Bed-

norz, Phys. Rev. B **36**, 401 (1987).
[5]M. Tuominen, A. M. Goldman, and M. L. Mecartney, Phys. Rev. B **37**, 548 (1988).
[6]Y. Yeshurun and A. P. Malozemoff, Phys. Rev. Lett. **60**, 2202 (1988).
[7]A. P. Malozemoff, L. Krusin-Elbaum, D. C. Cronemeyer, Y. Yeshurun, and F. Holtzberg, Phys. Rev. B **38**, 6490 (1988).
[8]Y. Yeshurun, A. P. Malozemoff, and F. Holtzberg (unpublished).
[9]P. H. Kes, P. Berghuis, S. Q. Guo, B. Dam, and G. M. Stallman, J. Less-Common. Met. **151**, 325 (1989).
[10]R. Griessen, C. F. J. Flipse, C. W. Hagan, J. Lensink, B. Dam, and G. M. Stollman, J. Less-Common Met. **151**, 39 (1989).
[11]M. Tinkham, Phys. Rev. Lett. **61**, 1658 (1988).
[12]P. W. Anderson, Phys. Rev. Lett. **9**, 309 (1962).
[13]D. Dew-Hughes, Cryogenics **28**, 675 (1988).
[14]C. P. Bean, Phys. Rev. Lett. **8**, 250 (1962).
[15]C. W. Hagen, R. Griessen, and E. Salmons (unpublished).
[16]C. W. Hagen and R. Griessen, in *High Temperature Superconductors,* edited by A. V. Narlikar (Nova, New York, in press).
[17]P. H. Kes, Physica C **153-155**, 1121 (1988).
[18]P. H. Kes, J. Aarto, J. van den Berg, C. J. van der Beek, and J. A. Mydosh, Supercond. Sci. Technol. (to be published).
[19]T. T. M. Palstra, B. Batlogg, R. B. van Dover, L. F. Schneemeyer, and J. V. Waszczak, Appl. Phys. Lett. **54**, 763 (1989).
[20]J. D. Hetlinger, A. G. Swanson, W. J. Skocpol, J. S. Brooks, J. M. Graybeal, P. M. Mankiewich, R. E. Howard, B. L. Straughn, and E. G. Burkhardt, Phys. Rev. Lett. **62**, 2044 (1989).
[21]E. Zeldov, N. M. Amer, G. Koren, A. Gupta, R. J. Gambino, and M. W. McElfresh, Phys. Rev. Lett. **62**, 3093 (1989).
[22]A. P. Malozemoff, T. K. Worthington, E. Zeldov, N. C. Yeh, M. W. McElfresh, and F. Holtzberg, in *Strong Correlations and Superconductivity,* Vol. 89 of *Springer Series in Physics,* edited by H. Fukuyama, S. Maekawa, and A. P. Malozemoff (Springer-Verlag, Heidelberg, 1989), p. 349.
[23]T. T. M. Palstra, B. Batlogg, R. B. van Dover, L. F. Schneemeyer, and J. R. Waszczak (unpublished).
[24]M. Nikolo and R. B. Goldfarb, Phys. Rev. B **39**, 6615 (1984).
[25]M. R. Beasley, R. Labush, and W. W. Webb, Phys. Rev. **181**, 682 (1969).
[26]W. A. Fietz, M. R. Beasley, J. Silcox, and W. W. Webb, Phys. Rev. **136**, A335 (1964).
[27]A. K. Ghosh, Youwen Xu, and M. Suenaga (unpublished).
[28]J. Friedel, P. G. DeGennes, and J. Matricon, Appl. Phys. Lett. **2**, 119 (1963).
[29]M. Tinkham and C. J. Lobb, *Solid State Physics,* edited by H. Ehrenreich and D. Turnbull (Academic, Boston, 1989), Vol. 42, p. 91.
[30]C. W. Hagen, E. Salomons, R. Griessen, and B. Dam (unpublished).
[31]Youwen Xu, M. Suenaga, J. Tafto, R. L. Sabatini, A. R. Moodenbaugh, and P. Zolliker, Phys. Rev. B **39**, 6667 (1989).
[32]Y. Zhu, M. Suenaga, Youwen Xu, R. L. Sabatini, and A. R. Moodenbaugh, Appl. Phys. Lett. **54**, 374 (1989).
[33]D. E. Farrell, B. S. Chandrasekhar, M. R. DeGuire, M. M. Fang, V. K. Kogan, J. R. Clem, and D. K. Finnemore, Phys. Rev. B **36**, 4026 (1987).
[34]D. E. Farrell, M. R. DeGuire, B. S. Chandrasekhar, S. Alterovitz, P. Aron, and M. M. Fang, Phys. Rev. B **35**, 8757 (1987).
[35]K. Yamafuji, T. Fujiyoshi, K. Toko, and T. Matsushita Physica **159C**, 743 (1989).
[36]M. Suenaga and M. Murakami (unpublished).
[37]D. O. Welch (unpublished).
[38]C. W. Hagen and R. Griessen, Phys. Rev. Lett. **62**, 2857 (1989).
[39]T. Matsushita, K. Fumaki, M. Takeo, and K. Yamafuji, Jpn. J. Appl. Phys. **26**, L1524 (1987).
[40]L. Ya. Vinnikov, L. A. Gurevich, G. A. Emel'chenko, and Yu. A. Osip'yan, Pisma Zh. Eksp. Teor. Fiz. **47**, 109 (1988) [JETP Lett. **47**, 131 (1988)].
[41]G. J. Dolan, G. V. Chandrashekhar, T. R. Dinger, C. Field, and F. Holtzberg, Phys. Rev. Lett. **62**, 827 (1989).